Proceedings of the 1st IEEE International
Conference on Nano/Micro Engineered and Molecular Systems
January 18 - 21, 2006, Zhuhai, China

Simulation and Analysis of Interfacial Wettability by Dissipative Particle Dynamics

Tzung-Han Lin[1], Wen-Pin Shih[1], Chuin-Shan Chen[2], and Yu-Tsung Chiu[3]

[1]*Department of Mechanical Engineering, National Taiwan University, Taipei, Taiwan.*
[2]*Department of Civil Engineering, National Taiwan University, Taipei, Taiwan.*
[3]*Materials and Chemical Engineering, Industrial Technology Research Institute, Hsinchu, Taiwan.*

***Abstract*—In this paper, we present a three-dimensional dissipative particle dynamics simulation, which is independent of the initial conditions, for analyzing the wettability on liquid-solid interfaces. The model parameters are constructed based on simulation optimization. The contact angle of a droplet on the solid platforms which possess different surface energy is simulated. The normalized factors indicate the parameters of the surface energy. By tuning the attractive and repulsive effects between the platform and the droplet, the contact angles with wide range are found at steady states. In simulation result, the linear relation between contact angle and the normalized factor is obtained. The proper repulsive factor in the paper is recommended to be 15 or 20. The ranges of the contact angles are from about 65 to 155 degrees. Moreover, the local density and the equation of state are applied for determining the droplet's self energy and compressibility. The simulation results will help us to predict the profile and internal physical behavior of a micro-droplet.**

Keywords-wettability; contact angle; dissipative particle dynamics; droplet; numerical simulation.

I. INTRODUCTION

Surface wettability is an important phenomenon for the development of microfluidic systems and biocompatible materials. The surface energy on the solid, liquid, and vapor interfaces is the intrinsic factor to dominate the surface wettability. In most applications, the interaction between solid and liquid is critical for the equilibrium state of the static droplet. Dissipative particle dynamics (DPD) becomes a feasible solution for these kinks of problems.

Different from molecular dynamics (MD), dissipative particle dynamics (DPD) has been developed as a mesoscopic simulation method. DPD has additional forces such as dissipative and random forces for simulating the hydrodynamic behavior [1, 2]. DPD has an improvement over conventional MD in computational efficiency by using meso-scale simulation. The thermodynamic and hydrodynamic behaviors of particles are simulated by statistical mechanics and maintain Brownian motions [3]. The dissipative force and the random force are correlated for the system to follow the principles of statistical mechanics corresponding to the simulated temperature. Instead of Eular algorithm, velocity-Verlet algorithm has been developed for integrating the equation of motion reliably. The integration schemes for variant conditions are adapted [4, 5]. The standard DPD is revealed for simulating single component [6] or multi-components. For example, two kinds of liquids with additional solid particles or particles with more parameters can be simulated [7]. The simulation for a pendant drop which considers the gravity effect is carried out by Clark et al. [8]. The measurement of the surface tension of liquid by a pendant drop test is also an important issue in simulating liquid-liquid particles [9].

The liquid-vapor coexistence DPD is developed with additional soft interaction between particles [10]. In the soft interaction, the attractive and repulsive forces are coupled in a conservative force. The liquid particles are constrained by the attractive forces and reach their equilibrium positions in long term. The liquid profile, which is a liquid-vapor coexistence layer, is determined when the simulated system achieves the steady state. Different kinds of responses of the conservative force have been introduced by Liu et al. [11]. Liu et al. adopted spline-based interaction of the conservative force to reproduce hydrodynamic behaviors. Their approach provided a convenient method for the design of interaction ranges and behaviors. In addition, multi-components models could be handled by specified response of spline. Different from Liu et al.'s method, the response of the conservative force in our method combines one straight line and one exponentially decayed curve.

In this paper, the solid surface in DPD is modeled as "freezing" particles which have no momentum. A conservative, repulsive force is added into the interaction between liquid particles so that the complicated boundary conditions of periodic space, as proposed by standard DPD, can be avoided. Unlike the pendant drop simulation, most DPD does not concern with the gravity effect [3]. In our work, the gravity term can be readily added and is optional. Furthermore, several kinds of equation of state (EOS) from [4] are also introduced into the simulation to model the vapor-liquid interface. Up to now, there is no report focusing on the numerical prediction of contact angle in the micro/nano-litter scale. We provide feasible DPD parameters for predicting the contact angle of the static droplet. A systematic simulation approach has been established by three-dimensional dissipative particle dynamics.

II. SIMULATION MODEL

A. Dissipative Particle Dynamics Simulations

In DPD models, the interactions between particles which are neighboring are simulated with pair forces. Each pair force

*Contacting Author: Tzung-Han Lin, Dept. of Mechanical Engineering, National Taiwan University, No.1, Sec. 4, Roosevelt Road, Taipei, Taiwan 106, (+886)-2-3366-2773, Email:d88522005@ntu.edu.tw.

($\mathbf{F}_{ij}$) for the particles i and j consists of a conservative force ($\mathbf{F}_{ij}^C$), a random force ($\mathbf{F}_{ij}^R$), and a dissipative force ($\mathbf{F}_{ij}^D$). A DPD particle is subject to all the pair forces from its neighboring particles. The driving force on particle i is represented as $\mathbf{f}_i$ in (1). The notation $\mathbf{F}_{ij}$ is the force exerted on the particle i due to the interaction with particle j. An opposite force acting on particle j will have the same magnitude but opposite direction, i.e. $\mathbf{F}_{ji} = -\mathbf{F}_{ij}$, due to the conservation of the momentum.

$$\mathbf{f}_i = \sum_{j \neq i} \mathbf{F}_{ij} = \sum_{j \neq i} (\mathbf{F}_{ij}^C + \mathbf{F}_{ij}^R + \mathbf{F}_{ij}^D) \tag{1}$$

The conservative force ($\mathbf{F}_{ij}^C$) is the soft interaction between particles and can be calculated by (2). The weighting functions in (3) and (4) are functions of the distances which are within specified distances. The magnitude of the conservative force (F_{ij}^C) is the function of the distance of two neighboring particles (Fig. 1). The factors A and B are used for tuning the maximum amplitudes for attractive and repulsive forces, respectively. It should be noted that the conservative force in conventional DPD only has the repulsive term, i.e. $A > 0$ and $B = 0$. A short range r_d, which is less than the cutoff r_c, is used for tuning the affected range of the repulsive force. In (2), r_{ij} is the length of the vector which starts from particle i to the particle j, $r_{ij} = r_j - r_i$, and $\mathbf{e}_{ij}$ is the unit vector, $\mathbf{e}_{ij} = r_{ij} / | r_{ij} |$. Different from conventional DPD, the conservative potential consists of attractive and repulsive terms. The attractive force which has $A < 0$ is linear to r_{ij}. The repulsive force which has $B > 0$ depends on the local densities and decays rapidly with increasing r_{ij}. In discrete computing, the local density (ρ_i) will be equal to the linear summation of finite particles as illustrated in (5).

$$\mathbf{F}_{ij}^C = A w_C(r_{ij}) \mathbf{e}_{ij} + B(\rho_i + \rho_j) w_{CD}(r_{ij}) \mathbf{e}_{ij} \tag{2}$$

$$w_C(r_{ij}) = \begin{cases} (1 - r_{ij}/r_c) & \text{if } r_{ij} < r_c \\ 0 & \text{otherwise} \end{cases} \tag{3}$$

$$w_{CD}(r_{ij}) = \begin{cases} (1 - r_{ij}/r_d) & \text{if } r_{ij} < r_d \\ 0 & \text{otherwise} \end{cases} \tag{4}$$

$$\rho_i = \frac{15}{2\pi r_d^2} \sum_j (1 - r_{ij}/r_d)^2 \tag{5}$$

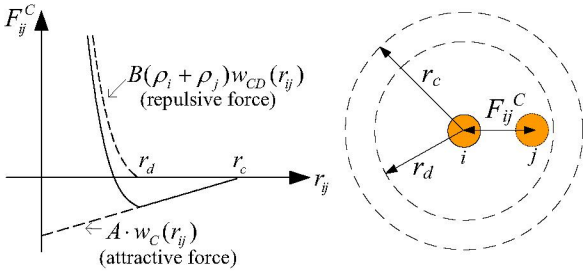

Figure 1. Pairwise conservative force has attractive and repulsive terms. A balanced distance of the pair exists when the magnitudes of attractive and repulsive forces are equivalent.

The random force, $\mathbf{F}_{ij}^R$, in (6) maintains the Brownian motion, and Gaussian random numbers are used. In a systemic simulation, the random number, ξ_{ij}, which generates normal distribution will have zero mean and unit variance. The pairwise random force also obeys Newton's third law, and particles i and j are subject to the same random force, i.e. $\xi_{ij} = \xi_{ji}$. Due to the pairwise random forces with Gaussian distribution, the angular momentum conserves. In (6), σ is a thermostat-rely coefficient. The dissipative force, $\mathbf{F}_{ij}^D$, presents the viscosity effect in the particle motion. $\mathbf{v}_i$ and $\mathbf{v}_j$ denote the velocities of particles i and j, respectively. The dissipative force depends on the current relative velocity, i.e. $\mathbf{v}_{ij} = \mathbf{v}_j - \mathbf{v}_i$. γ is the coefficient for the dissipative force. The weighting function in (8) is assumed the same as that in conservative force for simplicity. The fluctuation-dissipation theorem are adopted in (9) and (10), where k_B is the Boltzmann's constant, and T is temperature in DPD unit.

$$\mathbf{F}_{ij}^R = \sigma w_R(r_{ij}) \xi_{ij} \Delta t^{-1/2} \mathbf{e}_{ij} \tag{6}$$

$$\mathbf{F}_{ij}^D = -\gamma w_D(r_{ij}) (\mathbf{v}_{ij} \cdot \mathbf{e}_{ij}) \mathbf{e}_{ij} \tag{7}$$

$$w_R(r_{ij}) = w_C(r_{ij}) \tag{8}$$

$$\sigma^2 = 2\gamma k_B T \tag{9}$$

$$w_D(r_{ij}) = [w_R(r_{ij})]^2 \tag{10}$$

The DPD particles are driven by conservative, random, and dissipative forces and follow Newton's second law. Despite of these three forces, the gravity is ignored in micro/nano-scale simulation. Eular algorithm in (11) is typically used for the integration of the momentum. This algorithm is one of the conventional finite difference methods for integrating the velocity to obtain the particle positions. However, it may induce the numerical instability resulting from accumulated error.

$$\begin{aligned} \mathbf{r}_i(t + \Delta t) &= \mathbf{r}_i(t) + \mathbf{v}_i(t) \Delta t \\ \mathbf{v}_i(t + \Delta t) &= \mathbf{v}_i(t) + \mathbf{f}_i(t) \Delta t \\ \mathbf{f}_i(t + \Delta t) &= \mathbf{f}_i(\mathbf{r}_i(t + \Delta t), \mathbf{v}_i(t + \Delta t)) \end{aligned} \tag{11}$$

To improve the numerical stability, the velocity-Verlet algorithm in (12) is adopted in this work. Different from Eular algorithm, an intermediary velocity ($\tilde{\mathbf{v}}_i$) is used for the prediction of the velocity for the next integrated step. The momentum will be a function of the forces of two successive time steps. It should be noted that the time increment, Δt, in (6) is also critical to determine the thermostat.

$$\begin{aligned} \mathbf{r}_i(t + \Delta t) &= \mathbf{r}_i(t) + \mathbf{v}_i(t) \Delta t + \mathbf{f}_i(t) \cdot (\Delta t)^2 / 2 \\ \tilde{\mathbf{v}}_i(t + \Delta t) &= \mathbf{v}_i(t) + \mathbf{f}_i(t) \Delta t / 2 \\ \mathbf{f}_i(t + \Delta t) &= \mathbf{f}_i(\mathbf{r}_i(t + \Delta t), \tilde{\mathbf{v}}_i(t + \Delta t)) \\ \mathbf{v}_i(t + \Delta t) &= \mathbf{v}_i(t) + (\mathbf{f}_i(t) + \mathbf{f}_i(t + \Delta t)) \Delta t / 2 \end{aligned} \tag{12}$$

B. Simulated model

In order to simulate the surface wettability, the numerical models with a static droplet on a solid platform are designed. The contact angle of the simulated droplet is then extracted as a

index of the surface wettability. Initially, a solid cube is constructed with 20x20x2 in length, width and height, and a solid hemisphere is constructed with 12 in diameter. Then, the particles arranged as face centered cubic (FCC) with unit length are filled in these two models. The particles which denote the solid platform are freezing, and the particles which denote the static droplet are movable. Two kinds of particles are shown in Fig. 2, and there will be three kinks of parameters for pair forces. There are about 15000 liquid particles and 20000 solid particles. Because the solid particles are taken as the freezing particles, the parameter A_{SS} and B_{SS} for the pair forces are set to be zero, and the interaction between solid and solid particles can be neglected. The parameters of the pair forces for the liquid-liquid interaction are A_{LL} and B_{LL}, and the parameters for the liquid-solid interaction are A_{SL} and B_{SL}. Before starting the simulation, the liquid particles should be placed close enough to the solid particles, as shown in Fig. 2. In the simulation, there is no periodic boundary in any direction.

In the liquid-liquid interaction, the attractive force pulls the particles mutually to maintain the droplet shape by absorbing energy. If the attractive force between the interacting liquid particles becomes larger than the interfacial attraction, the interface tends to be hydrophilic. The dissipative and random forces are governed by the temperature according to (9). The temperature dominates particle motions in DPD algorithm, but the initial state of the droplet rarely affects the steady-state solutions. We carry out two fringe examples for demonstration, as shown in Fig. 3. Initially, the hemisphere-shaped cluster of particles with larger interactive attraction has overcome the interfacial attractive force from the platform. The other example is that the cluster with the same volume cannot conquer the attraction from the platform when larger interfacial attractive force is introduced. To shorten the simulation time, hemisphere-shape is used as the general initial condition for simulating the contact angle. After at least sixty thousand times integration, the steady state is obtained.

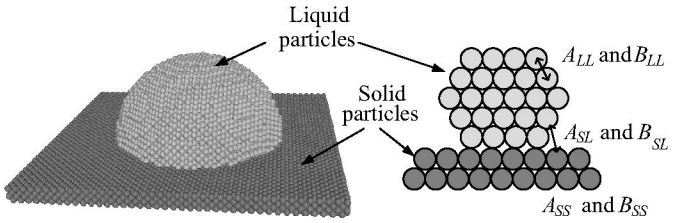

Figure 2. A static droplet on a solid platform is simulated with two kinds of DPD particles.

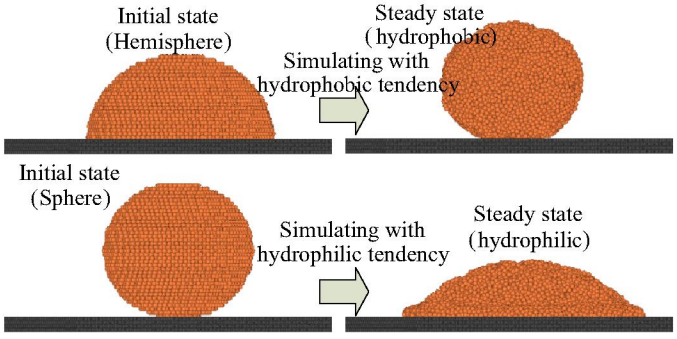

Figure 3. The simulation model is independent of the initial states.

III. Result and Discussion

The simulation parameters are listed in Table I. The interaction between the solid and liquid particles is only conservative force. Therefore, the interaction force between liquid particle i and solid particle j in (2) cab be rewritten as

$$\mathbf{F}_{ij}^{C} = A_{SL} w_C(r_{ij})\mathbf{e}_{ij} + 2B_{SL}\rho_i w_{CD}(r_{ij})\mathbf{e}_{ij} \tag{13}$$

The conservative force with attractive and repulsive effects induces different surface energies and dominates the surface wettability. For the interaction force, the repulsion is a function of the local densities of pair particles. If two particles are too close, the repulsive force will increase severely.

In this application, the determination of time increment for the integration depends on the stability of the global density ($\bar{\rho}$). We set a measuring box whose width is 2 inside the kernel of liquid particles. The measuring box is above the solid platform, and the minimum distance between the box and the platform is at least the cutoff distance. The global density is obtained by counting the numbers of particles inside the specified visual box. We assume the objective density is the mean of the local densities, i.e. $\langle \rho_i \rangle$. We take the mean of global densities at the first 200 integration steps and compare it with the mean of local densities. The velocity-Verlet algorithm is used in the integration, and the results in Fig. 4 indicate that the suitable time increment of the integration is about 0.009.

TABLE I. Simulation Parameters on Liquid-Liquid and Liquid-Solid Interface

liquid density	ρ	5.8
short range for repulsive force	r_d	0.75
cutoff distance	r_c	1.0
liquid-liquid attraction amplitude	A_{LL}	-40
liquid-liquid repulsion amplitude	B_{LL}	25
coefficient for random force	σ	7.45
coefficient for dissipative force	γ	27.75125
time step	Δt	0.009

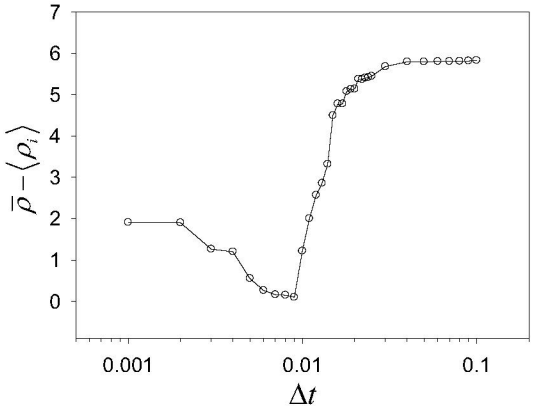

Figure 4. Determination of the time increment for integration by the stable global density.

In order to measure the contact angle of the 3D static droplet, 2D image processing technique is used (Fig. 5). In Fig. 5, the cross-sections of the droplets shown with different color-intensities indicate the value of local densities. The transitional profile exists between low density and high local density particles. The profile is fitted by a spline with five delegates. Inside the droplet, there is a quasi-uniform region with constant density, followed by a transitional region where the density decreases. Once the local density of the liquid particles is small enough, $\rho_i \cong 1$, the particle will be considered as in vapor phase. Because the equation of state (EOS) for each particle highly depends on its local density, the drawing for pressure is similar to the local density. The particles on the liquid-vapor interface show lower density and higher compressibility than the inner particles do. It is interesting to distinguish the interface of multi-components in mesocopic method. The contact angles are measured by at least fifty times for each simulating case. After simulation, the profile of the drop is slightly asymmetric. We measure the 3D droplet with different cross sections and take the peak of normal distribution. The contact angles versus the normalized parameters, i.e. $|A_{SL}|/B_{SL}$, are shown in Fig. 5. Second order polynomial curves, which fit the simulation results for each B_{SL}, indicate that the droplet has hydrophilic tendency with increasing the amplitude of attractive force ($|A_{SL}|$) and increasing the coefficient of repulsive force (B_{SL}). The wide contact angle range which is from 65° to 155° is obtained by the curve with B_{SL} = 15 or B_{SL} = 20, and their relations are linear. The contact angle on the line with B_{SL} = 15 or B_{SL} = 20 has a liner response with the normalized parameters. When B_{SL} = 15 or B_{SL} = 20, the contact angle is more predictable with different $|A_{SL}|$. The critical normalized parameter ($|A_{SL}|/B_{SL}$) which is neither hydrophobic nor hydrophilic is about 0.6 for B_{SL} = 20 and 0.7 for B_{SL} = 15.

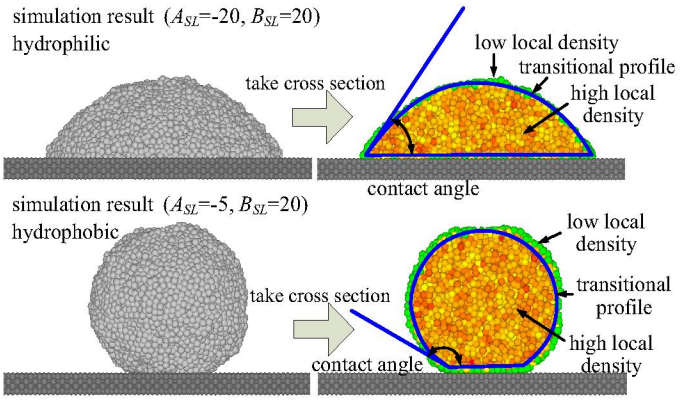

Figure 5. The transitional profile, which is between low local density particle and high local density particle, is the fundamental for measuring contact angle of discrete particles.

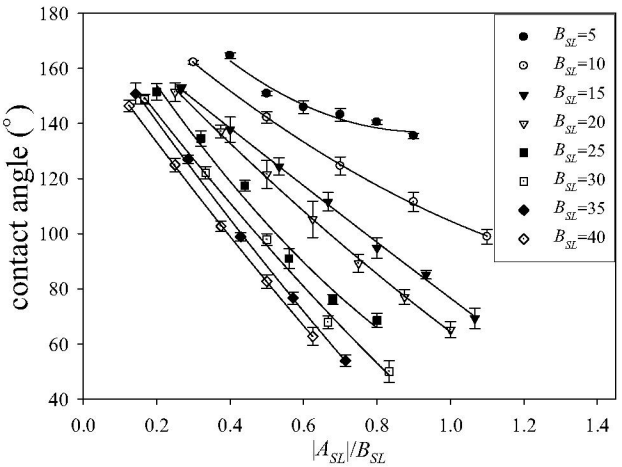

Figure 6. Contact angles in different normalized parameters.

IV. Conclusion

We have successfully implemented the DPD algorithm for realizing the hydrophobicity on liquid-solid interface. The static droplet sits on a solid platform and is subject to surface tensions. The shape of droplet holds due to equilibrium. Upon the convergence of the simulation, the droplet asymptotically reaches a steady state, and all of simulated particles move slightly with the remaining Brownian motion. Feasible parameters are provided for predicting contact angles of the static droplet which endures different surface energies.

References

[1] P. J. Hoogerbugge, and J. M. V. A. Koelman, "Simulating microscopic hydrodynamic phenomena with dissipative particle dynamics," Europhysics Letters, vol. 19, pp. 155–160, 1992.

[2] S. Y. Trofimov, E. L. F. Nies, and M. A. J. Michels, "Thermodynamic consistency in dissipative particle dynamics simulations of strongly nonideal liquids and liquid mixtures," Journal of Chemical Physics, vol. 17 (20), pp. 9383–9388, 2002.

[3] P. Espanol, "Statistical mechanics of dissipative particle dynamics," Europhysics Letters, vol. 30 (4), pp. 191–196, 1995.

[4] R. D. Groot, and P. B. Warren, "Dissipative particle dynamics: Bridging the gap between atomistic and mesoscopic simulation," Journal of Chemical Physics, vol. 107 (11), pp. 4423–4435, 1997.

[5] I. Vattulainen, M. Karttunen, G. Besold, and J. M. Polson, "Integration schemes for dissipative particle dynamics simulations: From softly interacting systems towards hybrid models," Journal of Chemical Physics, vol. 116 (10), pp. 3967–3979, 2002.

[6] D. Frenkel, and B. Smit, Understanding molecular simulation: from algorithms to applications, San Diego: Academic Press, 2002, pp. 465–478.

[7] J. L. Jones, M. Lal, J. N. Ruddock, and N. A. Spenley, "Dynamics of a drop at a liquid/solid interface in simple shear fields: A mesoscapic simulation study," Faraday Discuss, vol. 112, pp. 129–142, 1999.

[8] A. T. Clark, M. Lal, J. N. Ruddock, and P. B. Warren, "Mesoscopic simulation of drops in Gravitational and Share Fields," Langmuir, vol. 16, pp. 6342–6350, 2000.

[9] C. E. Stauffer, "The measurement of surface tension by pendant drop technique," The Journal of Physical Chemistry, vol. 69 (6), pp. 1933–1938, 1965.

[10] P. B. Warren, "Vapor-liquid coexistence in many-body dissipative particle dynamics," Physical Review E, vol. 68 (8), pp.066702, 2003.

[11] M. Liu, P. Meakin, and H. Huang, "Dissipative particle dynamics with attractive and repulsive particle interactions," Physics of Fluids, vol. 18, pp. 017101–13, 2006.